

289. Unusual Features in the ESR.
Spectra of 1,6-Methano[10]annulene Radical Anion.
A Modified McConnell Equation for Non-Planar π -Radicals

by **F. Gerson**¹⁾, **K. Müllen**¹⁾ and **E. Vogel**²⁾

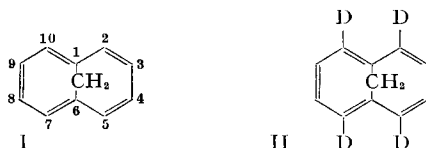
Physikalisch-Chemisches Institut der Universität Basel,
 Klingelbergstrasse 80, 4056 Basel, Switzerland, and
 Organisch-Chemisches Institut der Universität Köln,
 Zülpicher Strasse 47, 5 Köln, Germany

(15. X. 71)

Summary. ESR. spectra of the radical anions of 1,6-methano[10]annulene (I) and its 2,5,7,10-tetradeuterio derivative II are reported for a temperature range of over 100°. The abnormally small magnitudes of the α -proton coupling constants are attributed to the deviation of the ten-membered π -perimeter from planarity; an extension of the *McConnell* equation is proposed to achieve agreement between theory and experiment. It is suggested that the marked temperature-dependence of the ESR. spectra arises from slight changes in geometry which for I^\ominus should have a more pronounced effect on the α -proton coupling constants than for planar π -radicals.

Several years ago, we reported the ESR. data for the radical anions of 1,6-methano[10]annulene (I) and some of this deuterio derivatives [1]. The coupling constants of the α -protons³⁾ in I^\ominus were found to deviate strongly from the expected values. Later investigations also revealed that the ESR. spectrum of I^\ominus , which was previously observed at -70° , is markedly temperature dependent.

In the present paper we report the ESR. data for I^\ominus and its 2,5,7,10-tetradeuterio derivative II^\ominus over a range of more than 100°C.⁴⁾ We also discuss the effect of non-planarity of the ten-membered perimeter on the α -proton coupling constants and attempt to rationalize their temperature dependence in terms of changes in geometry.



Results. – *Radical anion of 1,6-methano[10]annulene (I).* Fig. 1 illustrates the effect of temperature variation on the ESR. spectra of I^\ominus in 1,2-dimethoxyethane (DME) with Na^\oplus as counter-ion.⁵⁾ Before the observed changes in the spectra are

¹⁾ Universität Basel.

²⁾ Universität Köln.

³⁾ In ESR. spectroscopy, protons are denoted by the Greek letters α , β , γ ... according to whether they are linked to a π -electron center *via* 0, 1, 2 ... sp^3 -hybridized carbon atoms. The eight protons attached to the ten-membered ring in I^\ominus thus represent α -protons, whereas the two protons in the methylene bridging group must be considered as β -protons [2].

⁴⁾ A selection of these ESR.-data has appeared in a recent review on non-benzenoid radical ions [3].

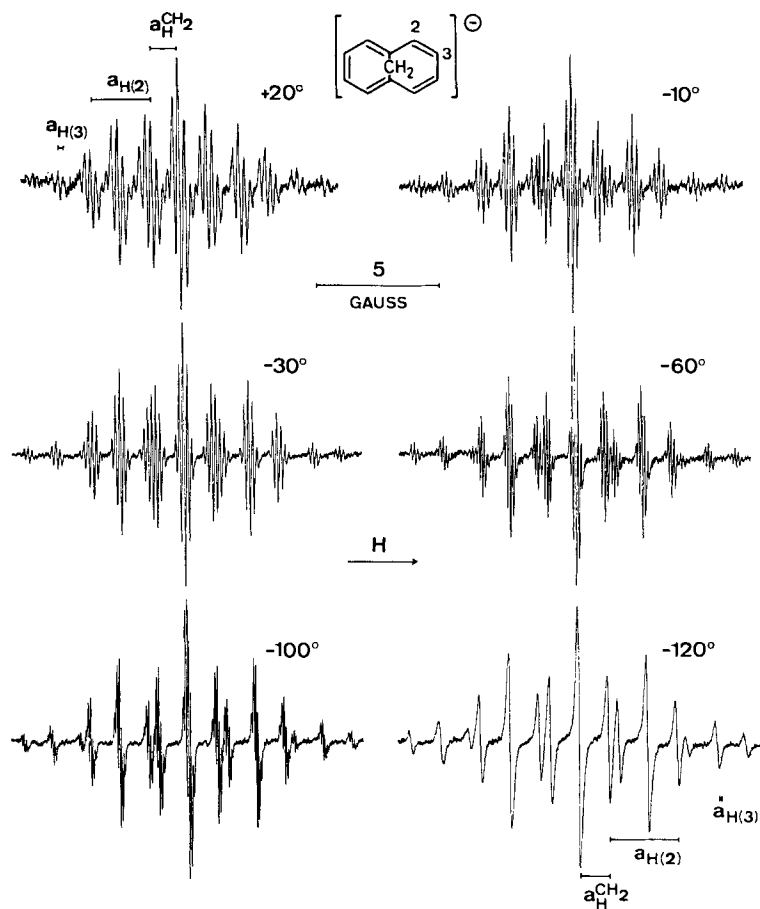


Fig. 1. ESR spectra of the radical anion I^{\ominus} at various temperatures
Solvent: DME; counter-ion: Na^{\oplus}

analysed in terms of changes in the proton coupling constants, two points should be noted:

1. The spectra do not exhibit a measurable hyperfine splitting due to the ^{23}Na nucleus, in contrast to the spectra of I^{\ominus} studied under different conditions where such ^{23}Na or ^{39}K splitting is always present (see below).

2. For temperatures above $-60^{\circ}C$, the same spectra as those shown in Fig. 1 are obtained – albeit with slightly decreased resolution – by electrolytic generation of I^{\ominus} in *N,N*-dimethylformamide with $(C_2H_5)_4N^{\oplus}ClO_4^{\ominus}$ as supporting salt. In this system I^{\ominus} is considered to be non-associated with the counter-ion.

We conclude that I^{\ominus} is not associated with Na^{\oplus} in DME above -60° ; since the polarity of the solvent increases at lower temperatures, this conclusion is even more valid for the spectra recorded below -60° . Consequently, one might anticipate that the striking spectral changes do not arise from ion pairing phenomena.

In Table 1 the pertinent coupling constants $a_{H(2)}$, $a_{H(3)}$, and $a_H^{CH_2}$ are listed for the two sets of four equivalent α -protons³⁾ in positions 2, 5, 7, 10 and 3, 4, 8, 9, and for the pair of equivalent methylene β -protons³⁾. The signs of these values will be considered in the Discussion and only their absolute magnitudes – as determined from the ESR. spectra – are dealt with at present.

The plots of $|a_{H(2)}|$, $|a_{H(3)}|$, and $|a_H^{CH_2}|$ vs. temperature (T) are presented in Fig. 2. In the range of investigation an almost linear relationship is observed, the

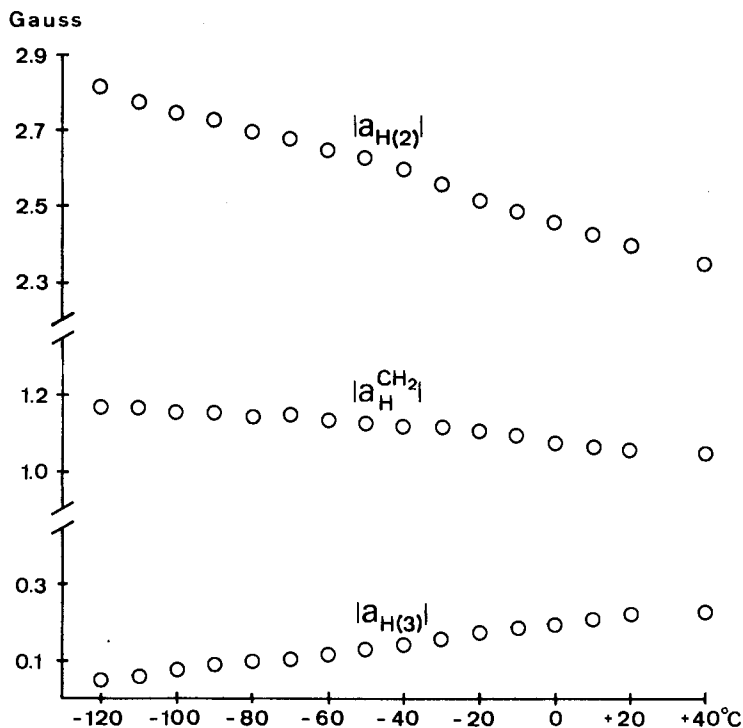


Fig. 2. Coupling constants of the protons in I^{\ominus} vs. temperature

slopes of the lines being $d|a_{H(2)}|/dT = -2.9 \pm 0.3$; $d|a_{H(3)}|/dT = +1.2 \pm 0.1$, and $d|a_H^{CH_2}|/dT = -0.8 \pm 0.2$ milligauss/degree.

Relative to the values measured at -40° (range centre), the changes per 100° amount to $-11(\pm 1)\%$, $+85(\pm 10)\%$ and $-7(\pm 1)\%$ for $|a_{H(2)}|$, $|a_{H(3)}|$ and $|a_H^{CH_2}|$, respectively. The absolute magnitudes of $a_{H(2)}$ and $a_H^{CH_2}$ thus decrease, whereas that of $a_{H(3)}$ increases with rising temperature.

Radical anion of 2,5,7,10-tetradeuterio-1,6-methano[10]annulene(II): Fig. 3 shows the ESR. spectra of II^{\ominus} observed at various temperatures in DME with Na^{\oplus} as counter-ion. Table 2 contains the values $|a_{D(2)}|$, $|a_{H(3)}|$ and $|a_H^{CH_2}|$ for the four equivalent α -deuterons in the positions 2, 5, 7, 10, the four equivalent α -protons in 3, 4, 8, 9, and the two equivalent methylene β -protons. The almost linear temperature

⁵⁾ For the spectra taken below -90° a few drops of tetrahydrofuran (THF) were added to prevent solidification of DME.

Table 1. *Coupling constants of protons in the radical anion I[⊖]*Solvent: DME; counter-ion: Na[⊕]; temperature range: –120 to +40°C⁴⁾Experimental error: $|a_{H(2)}|$: ± 0.02 ; $|a_{H(3)}|$: ± 0.005 ; $|a_{H}^{CH_2}|$: ± 0.01

Temperature in °C	Coupling constants in gauss		
	$ a_{H(2)} $	$ a_{H(3)} $	$ a_{H}^{CH_2} $
–120	2.82	<0.055	1.17
–110	2.78	0.061	1.17
–100	2.75	0.073	1.16
–90	2.73	0.087	1.16
–80	2.70	0.099	1.15
–70	2.68	0.108	1.15
–60	2.65	0.122	1.14
–50	2.63	0.130	1.13
–40	2.60	0.142	1.12
–30	2.56	0.158	1.12
–20	2.53	0.175	1.11
–10	2.49	0.187	1.10
0	2.46	0.198	1.08
+10	2.43	0.213	1.07
+20	2.40	0.226	1.06
+40	2.35	0.240	1.05

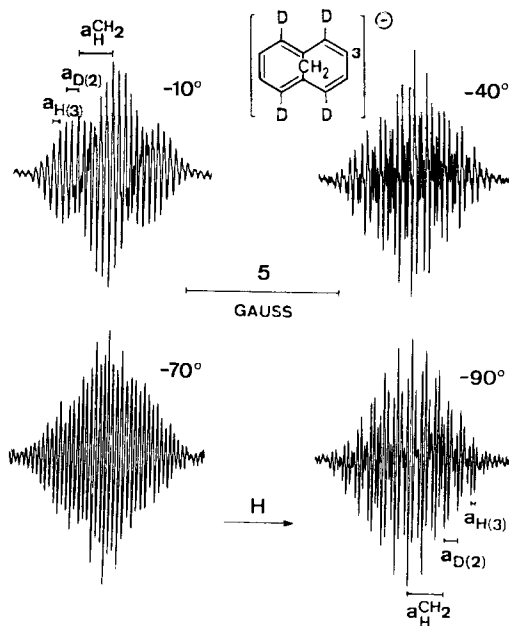
Fig. 3. *ESR spectra of the radical anion I1[⊖] at various temperatures*Solvent: DME; counter-ion: Na[⊕]

Table 2. Coupling constants of protons and deuterons in the radical anion II^\ominus Solvent: DME; counter-ion: Na^\oplus ; temperature range: -90 to $+22^\circ C$ Experimental error: $|a_{D(2)}|$ and $|a_{H(3)}|$: ± 0.005 ; $|a_H^{CH_2}|$: ± 0.01

Temperature in $^\circ C$	Coupling constants in gauss		
	$ a_{D(2)} $	$ a_{H(3)} $	$ a_H^{CH_2} $
-90	0.429	0.113	1.16
-80	0.427	0.127	1.15
-70	0.423	0.141	1.14
-60	0.420	0.153	1.14
-50	0.412	0.162	1.13
-40	0.408	0.173	1.13
-30	0.405	0.190	1.12
-20	0.401	0.195	1.11
-10	0.396	0.202	1.10
0	0.393	0.211	1.09
+10	0.389	0.219	1.08
+20	0.380	0.238	1.07

dependence of these values can be described by $d|a_{D(2)}|/dT = -0.45 \pm 0.05$; $d|a_{H(3)}|/dT = +1.1 \pm 0.1$ and $d|a_H^{CH_2}|/dT = -0.8 \pm 0.1$ milligauss/degree.

Changes per $100^\circ C$ relative to the values at -40° amount to $-11(\pm 2)\%$, $+65(\pm 10)\%$, and $-7(\pm 1)\%$ for $|a_{D(2)}|$, $|a_{H(3)}|$ and $|a_H^{CH_2}|$, respectively.

A comparison of the data for I^\ominus and II^\ominus allows one to make the following comments:

1. The ratio $|a_{D(2)}|/|a_{H(2)}| = 0.158 \pm 0.002$ remains almost constant throughout the whole temperature range of investigation. This constancy is reflected by the equal relative changes $d|a_{H(2)}|/dT$ and $d|a_{D(2)}|/dT$.

2. The $|a_{H(3)}|$ values for I^\ominus and II^\ominus differ significantly, in particular at lower temperatures. However, differences of the same order of magnitude (0.01 to 0.03 gauss) have also been observed for the coupling constants of α -protons at the corresponding non-deuterated positions in the radical anions of naphthalene and its deuterio derivatives [4].

3. Deuteration does not affect the $|a_H^{CH_2}|$ values.

The ESR. data for II^\ominus are thus fully in line with those for I^\ominus , and only the latter need be considered in the Discussion.

Association with alkali metal cations. Use of tetrahydrofuran (THF) instead of DME as a solvent and simultaneous replacement of Na^\oplus by K^\oplus as counter-ion result in a radical anion of 1,6-methano[10]annulene (I) which is associated with the alkali metal cation. The association is favoured both by the smaller solvating power of THF, as compared to DME, and by the weaker solvation of K^\oplus relative to Na^\oplus). The evidence for a relatively strong ion-pairing of I^\ominus with K^\oplus in THF solution is given by an additional ^{39}K hyperfine splitting which can be observed even at the lowest temperature investigated ($-120^\circ C$). Figure 4 shows an ESR. spectrum taken at $-30^\circ C$ in which a fourfold increase in the number of lines due to a ^{39}K splitting of 0.08 ± 0.01

⁶⁾ In the case of hydrocarbon radical anions such as I^\ominus , the association usually becomes stronger as the radius of the counter-ion increases, because the solvation (which competes with ion-pairing) decreases with increasing size of the cation.

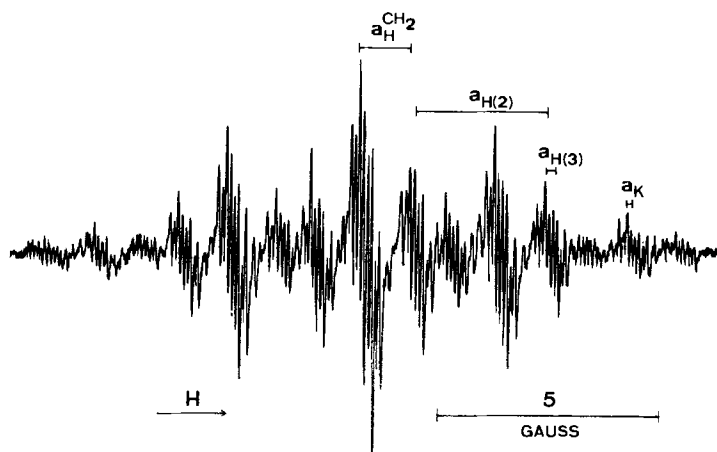


Fig. 4. ESR spectrum of the radical anion I^{\ominus} associated with its counter-ion K^{\oplus}
Solvent: THF; temp.: -30°

gauss is clearly evident. The presence of two small, temperature-dependent coupling constants $a_{H(3)}$ and a_K (absolute magnitude of the order 0.1 gauss) greatly complicates the analysis of the spectra. Therefore, only the two larger coupling constants $a_{H(2)}$ and $a_H^{CH_2}$ have been measured throughout the whole temperature range. In contrast to the $|a_H^{CH_2}|$ values, which do not significantly deviate from those listed in Table 1 for the non-associated radical anion, a remarkable difference in $|a_{H(2)}|$ is observed as a consequence of ion-pairing. Since this difference (0.3 to 0.4 gauss) persists throughout the whole temperature range (-120° to $+20^{\circ}$), the plot of $|a_{H(2)}|$ vs. T for the ion-paired species I^{\ominus} can be represented by a line which is almost parallel to that found for the non-associated radical anion. This result is illustrated by Figure 5 which shows the plots of $|a_{H(2)}|$ vs. T for the solvent/counter-ion systems DME/ Na^{\oplus} and THF/ K^{\oplus} as well as for the two other combinations DME/ K^{\oplus} and THF/ Na^{\oplus} .

As might be expected, the systems DME/ K^{\oplus} and THF/ Na^{\oplus} are intermediate between DME/ Na^{\oplus} and THF/ K^{\oplus} as far as the association of I^{\ominus} with the counter-ion is concerned. Whereas at

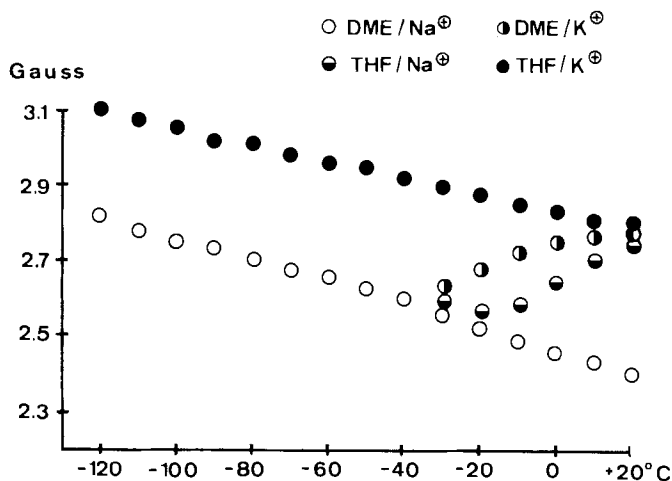
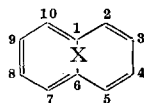


Fig. 5. Coupling constant $|a_{H(2)}|$ for I^{\ominus} in four solvent/counter-ion systems vs. temperature
At $T < -40^{\circ}$ the points for DME/ K^{\oplus} and THF/ Na^{\oplus} coincide with those for DME/ Na^{\oplus}

$T < -40^\circ$, the ESR. spectra for the intermediate systems are identical with those of the non-associated radical anion (DME/Na[⊕]), conversion to an ion-paired species (THF/K[⊕]) occurs at higher temperatures. Such a conversion is not only manifested by an appearance of an additional ²³Na or ³⁹K splitting in the ESR. spectra, but also reflected by the plots of $|a_{\text{H}(2)}|$ vs. T shown in Figure 5. Whereas at $T < -40^\circ$ the values $|a_{\text{H}(2)}|$ for DME/K[⊕] and THF/Na[⊕] are equal to those for DME/Na[⊕], they approach those for THF/K[⊕] at room temperature. In the transition range ($-40^\circ < T < +20^\circ$) a decrease in the $|a_{\text{H}(2)}|$ value with rising temperature is opposed by a concomitant increase due to stronger association.



III, when X = NH

IV, when X = O

Radical anions of 1,6-imino- and 1,6-oxido[10]annulenes (III and IV, respectively). The ESR. spectra of the two radical anions III[⊖] and IV[⊖], which exhibit proton coupling constants $a_{\text{H}(\mu)}$ comparable to those measured for I[⊖], were also studied at -70° [1] [5]. Investigations of III[⊖] and IV[⊖] at higher temperatures are impeded by the low stability of these radical anions. In particular, the rapid decay of IV[⊖] above -70° precludes any definite conclusions that might be made regarding the temperature dependence of the spectra. On the other hand, the radical anion III[⊖] is sufficiently stable up to -20° , and ESR. studies are feasible below this temperature. The results of such studies (solvent: DME; counter-ion: Na[⊕] or K[⊕]) indicate a decrease in the values $|a_{\text{H}(\mu)}|$ for $\mu = 2, 5, 7, 10$ and an increase for $\mu = 3, 4, 8, 9$. The coupling constants of the ring protons in III[⊖] thus display a similar temperature dependence as the corresponding values for I[⊖].

Discussion. – *Preliminary remarks.* The temperature dependent changes in the coupling constants of the α -protons in I[⊖], $a_{\text{H}(2)}$ and $a_{\text{H}(3)}$, exceed by far those usually found for hydrocarbon π -radicals. In Fig. 6, a comparison is made between the values

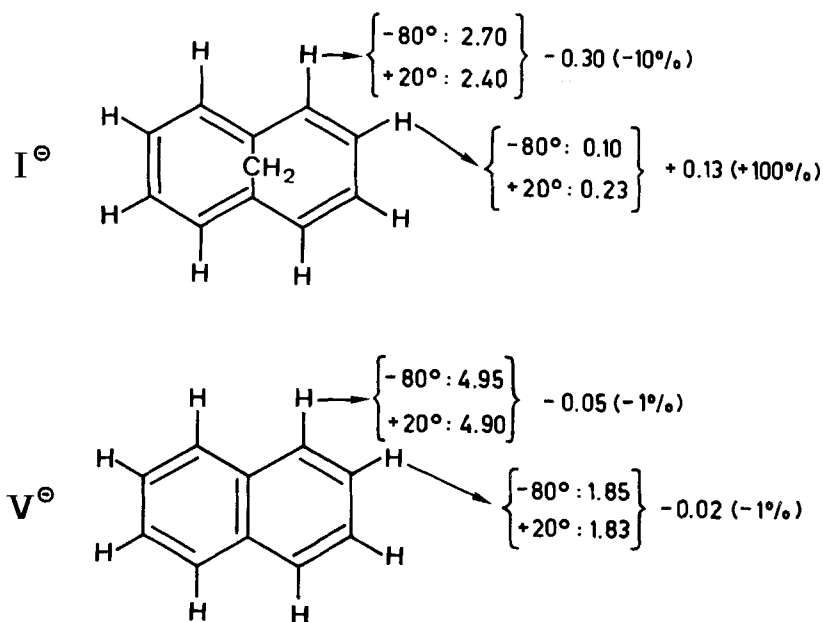


Fig. 6. Coupling constants of the α -protons in the radical anions I[⊖] and V[⊖] at $+20$ and -80°
Absolute values in gauss

$|a_{\text{H}(\mu)}|$ for I^\ominus and the naphthalene radical anion V^\ominus . It is evident that the relative changes for I^\ominus are one or two orders of magnitude larger than the analogous changes for V^\ominus . As will be shown below, a comparison between the coupling constants of the α -protons³⁾ in I^\ominus and V^\ominus is also informative in another respect: although theory requires similar values $a_{\text{H}(\mu)}$ for the corresponding α -protons in the two radical anions, the experimental values differ considerably. In our opinion, the reasons for this difference are closely related to those responsible for the temperature dependence of the α -proton coupling constants; they will be discussed in the section dealing with effects of non-planarity. Prior to this discussion, however, it is desirable to consider whether ‘orbital mixing’ in I^\ominus could be the source of the temperature dependence.

Orbital mixing. Coupling constants of α -protons in a few hydrocarbon π -radicals having a near-degenerate ground state are known to exhibit a temperature dependence comparable to that observed for I^\ominus [6] [7]. In such π -radicals, thermal mixing of two energetically close orbitals results in temperature dependent π -spin populations q_μ at the carbon centers μ , and hence, by virtue of the *McConnell* equation (1) [8] in

$$a_{\text{H}(\mu)} = Q \cdot q_\mu, \quad (1)$$

temperature dependent $a_{\text{H}(\mu)}$ values. Since the bridged [10]annulene **I** can be treated as a ten-membered perimeter, in which the orbital degeneracies are removed by a perturbation [1] [9], it is tempting to assume that thermal mixing leads to the observed changes in the values $a_{\text{H}(\mu)}$ for I^\ominus as well.

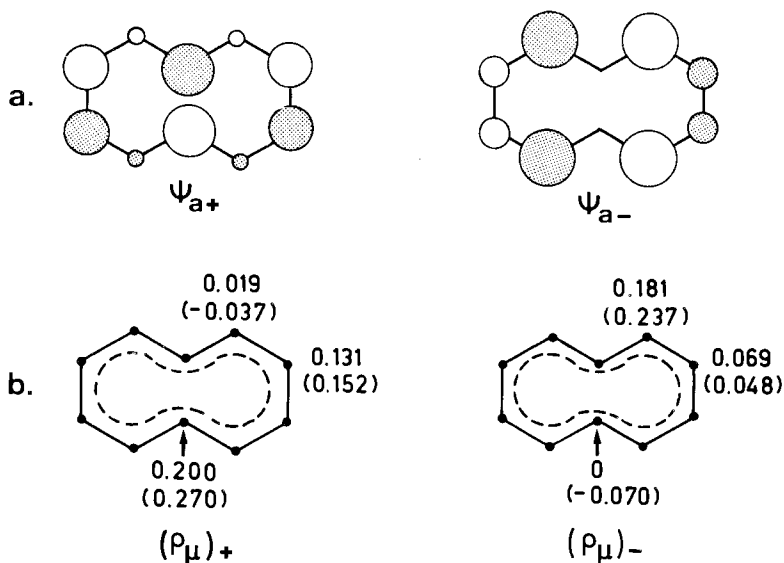


Fig. 7. a. The degenerate lowest antibonding orbitals ψ_{a+} and ψ_{a-} of the ten-membered perimeter. "Plus" signifies symmetric and "minus" antisymmetric relative to a mirror plane which passes through the centers 1 and 6 and is perpendicular to the plane of the perimeter. The radii of the circles are proportional to the absolute values of the LCAO-coefficients; blank and dotted areas refer to relative signs of these coefficients.

b. π -spin populations $(q_\mu)_+$ and $(q_\mu)_-$ for the single occupancy of ψ_{a+} and ψ_{a-} , respectively

Values calculated by the *McLachlan* procedure [10] are given in parentheses

Fig. 7a presents the degenerate lowest antibonding orbitals $\psi_{a+} = 0.447 (\phi_1 - \phi_6) - 0.138 (\phi_2 - \phi_5 - \phi_7 + \phi_{10}) - 0.362 (\phi_3 - \phi_4 - \phi_8 + \phi_9)$ and $\psi_{a-} = 0.425 (\phi_2 + \phi_5 - \phi_7 - \phi_{10}) - 0.263 (\phi_3 + \phi_4 - \phi_8 - \phi_9)$ of the ten-membered perimeter. In Fig. 7b, the HMO and *McLachlan* [10] spin populations⁷⁾, $(\rho_\mu)_+$ and $(\rho_\mu)_-$, are given for the single occupancy of ψ_{a+} and ψ_{a-} , respectively. From the ESR. data ($|a_{H(2)}| \gg |a_{H(3)}|$) one readily concludes that the π -spin population in I^\ominus is distributed according to $(\rho_\mu)_-$, i.e. the orbital ψ_{a-} has lower energy than its counterpart ψ_{a+} and thus determines the spin distribution in I^\ominus . An admixture of $(\rho_\mu)_+$ to $(\rho_\mu)_-$ is, however, possible if the two orbitals differ only slightly in their energies (near-degeneracy) so that ψ_{a+} can contribute to the π -spin population (orbital mixing) [11]. Moreover, if the relevant energy gap is small enough to be comparable to the thermal energy, the amount of the admixture will increase with increasing temperature (thermal mixing) [7] [11]. Since $(\rho_2)_+ < (\rho_2)_-$ and $(\rho_3)_+ > (\rho_3)_-$, this increase would result in a smaller ρ_2 and a larger ρ_3 π -spin population, in agreement with the parallel temperature dependent changes found for $|a_{H(2)}|$ and $|a_{H(3)}|$.

However, these arguments in favour of the thermal mixing are invalidated by the prerequisite that the gap between the energies of ψ_{a+} and ψ_{a-} should be smaller than 0.05 eV. The values calculated for π -electron (PPP[12]) and all valence electron (INDO [13]) models are at least one order of magnitude larger than those required by an effective thermal mixing. This result can be expected even in terms of a qualitative treatment of the perimeter model, because the bridging in 1,6-methano[10]annulene should markedly affect the energies of the perimeter orbitals [14]. Consequently, the orbital mixing is not likely to be the 'mechanism' responsible for the temperature dependent coupling constants of the α -protons in I^\ominus and an alternative 'mechanism' must be considered.

Adequacy of the McConnell equation. Use of eq. (1) with $\rho_\mu \approx (\rho_\mu)_-$ (Fig. 7b) and $Q = -20$ to -30 gauss [15] yields coupling constants $a_{H(2)} = -4$ to -6 and $a_{H(3)} = -1$ to -2 gauss. Comparison of these values with those found experimentally for I^\ominus (Table 1) shows that the latter have absolute magnitudes reduced by 1 to 3 gauss relative to the former. The reduction is also evident from the numbers in Fig. 6. Since, in the HMO model, the lowest antibonding orbital of V is identical with ψ_{a-} , the coupling constants of the α -protons in I^\ominus are expected to be as large as the corresponding values for V^\ominus . Clearly, this expectation is not borne out by experiment.

The striking disagreement between theory and experiment cannot be due to any substantial reduction in the π -spin populations ρ_μ in I^\ominus relative to the calculated values $(\rho_\mu)_-$. MO models at various levels of sophistication (*McLachlan* [10], INDO [13]) indicate that neither the perturbation due to the bridging group nor the moderate deviation of the ten-membered ring from planarity (the twisting angle of two consecutive $2p\pi$ -orbitals out of alignment should not exceed 30° [16]) essentially alter the π -spin populations ρ_μ . This prediction is supported by the ESR. data for the methylene β -protons and ^{13}C nuclei of I^\ominus which – in contrast to the α -proton coupling constants $a_{H(\mu)}$ – are consistent with the expected values.

$$a_{\text{H}}^{\text{CH}_n} = B \cdot \rho_\mu \cdot \langle \cos^2 \theta \rangle \quad (2)$$

⁷⁾ The *McLachlan* parameter λ [10] was given its usual value of 1.2.

Thus, use of the equation (2) [17] for the β -protons with $B = +45$ gauss, $\theta = 60^\circ$ and $\rho_\mu = -0.14$ ⁸⁾ leads to $a_{\text{H}}^{\text{CH}_2} = -1.5$ gauss, which is in fair agreement with the experimental value $|a_{\text{H}}^{\text{CH}_2}| = 1.05 - 1.17$ gauss. (Note that eq. (2) predicts a negative sign for $a_{\text{H}}^{\text{CH}_2}$.)

Likewise, the coupling constants $|a_{\text{C}(2)}| = 6.9$ and $|a_{\text{C}(1)}| = 6.4$ gauss found for ¹³C nuclei in the carbon centers 2, 5, 7, 10 and 1, 6, respectively (see Appendix) are fairly close to the corresponding numbers 7.3 and 5.6 gauss for V[⊖] [19], despite the striking differences in the values $|a_{\text{H}(\mu)}|$. Consequently, it may be deduced that the π -spin populations ρ_μ in I[⊖] are comparable to those in V[⊖] and can be reasonably represented by the values $(\rho_\mu)_-$ given in Fig. 7b.

Since the apparent reduction in $|a_{\text{H}(2)}|$ and $|a_{\text{H}(3)}|$ for I[⊖] cannot be due to any substantial lowering of the π -spin populations ρ_μ , one may argue that the absolute value of the parameter Q in eq. (1) should be reduced in order to achieve agreement with the experimental data. However, the values $|Q|$ required to reproduce the data $|a_{\text{H}(2)}|$ and $|a_{\text{H}(3)}|$ are ~ 10 and ~ 1 gauss, respectively. These numbers seem quite unrealistic and thus the question must be posed whether the *McConnell* equation as formulated by (1) is still adequate to account for the coupling constants of the α -protons in I[⊖].

Effects of non-planarity. The *McConnell* equation implies that π - σ spin polarisation is the only essential mechanism for the transfer of spin from the $2p\pi$ -carbon-AO's to the $1s$ -AO's of the adjacent α -hydrogens. It is therefore not surprising that eq. (1) has proved to be quite adequate for planar π -radicals in which the π - σ separation is justified and a direct transfer of spin by delocalisation may be neglected. On the other hand, in non-planar π -radicals such as I[⊖], the π - σ delocalisation is appreciable, and significant $1s$ -spin populations can be generated at the α -hydrogens by a direct transfer of spin from the $2p\pi$ -AO's of the carbon atoms.

A fragment comprising a carbon π -center μ , an attached α -hydrogen, and two neighbouring centers ν and ν' is depicted in Fig. 8b. The coupling constants $a_{\text{H}(\mu)}$ of the ring proton in a non-planar π -radical can be expressed as equation (3) [20] where the

$$a_{\text{H}(\mu)} = Q \cdot \rho_\mu + A \cdot \rho_\mu \langle \cos^2 \varphi \rangle + B' \rho_\nu \langle \cos^2 \theta_{\mu\nu} \rangle + B' \rho_{\nu'} \langle \cos^2 \theta_{\mu\nu'} \rangle \quad (3)$$

A - and B' -terms are comparable to the right hand side of eq. (2). Accordingly, the parameters A and B' , and the angles φ , $\theta_{\mu\nu}$ and $\theta_{\mu\nu'}$ have similar meanings to the corresponding quantities B and θ in eq. (2), as evident from Fig. 8.

The extension of eq. (1) by adding the A - and B' -terms allows for the non-planarity of the π -system in the neighbourhood of the relevant center μ . Clearly, for a planar π -radical, $\varphi = \theta_{\mu\nu} = \theta_{\mu\nu'} = 90^\circ$ so that the three additional terms vanish and eq. (3) reduces to eq. (1).

Evaluation of the parameters A and B' , both of which must be positive, is difficult. Consideration of the distance between the α -proton and the pertinent π -spin population suggests an order $A \gg B' > B$. If B is given a value of $+45$ gauss⁸⁾, then B' should amount to at least $+50$

⁸⁾ The value $1/2 B = 22.4$ gauss was derived from the coupling constants of the β -protons in the radical anions of dimethyl-naphthalenes [18]. The dihedral angle $\theta = 60^\circ$ (Figure 8a) has been estimated from a molecular model of I. The π -spin population $\rho_\mu = -0.14$ was taken as the sum of the *McLachlan* values $\rho_1 + \rho_6 = -0.14$ at the two bridged centers 1 and 6 (Figure 7b), which are linked by the methylene group.

gauss [20], whereas the value of A could be as large as +100 to +150 gauss. Since Q is negative, the A -term always has a sign opposite to that of the *McConnell* term. The sign of the B' -terms,

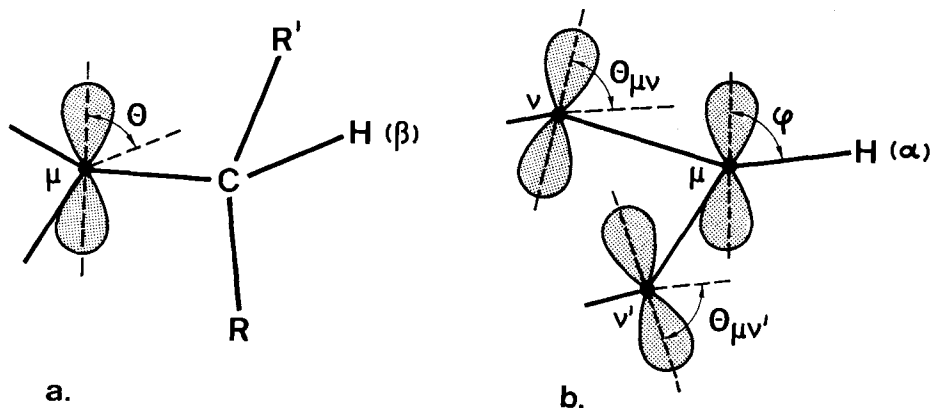


Fig. 8. Schematic representations of:

- a. Alkyl substituent at a center μ
 b. Fragment containing a proton-bearing center μ and two adjacent centers ν and ν'

on the other hand, can be either opposite or the same as that of the *McConnell* term, according to whether the π -spin populations ρ_ν and $\rho_{\nu'}$ at the neighbouring centers are the same or opposite in sign to ρ_μ . Consequently, the A -term always leads to reduction in the value $a_{H(\mu)}$ from that calculated by means of eq. (1), whereas the inclusion of the B' -terms can result in either a decrease (the same sign of ρ_μ and $\rho_\nu, \rho_{\nu'}$) or increase in $a_{H(\mu)}$ (opposite signs of ρ_μ and $\rho_\nu, \rho_{\nu'}$) [20].

Despite the uncertainty with regard to the values of A and B' , the contributions to the coupling constants $a_{H(2)}$ and $a_{H(3)}$ can be qualitatively discussed in terms of eq. (3), using the predicted π -spin populations $\rho_\mu = (\rho_\mu)_-$ (Fig. 7b). Since $|\rho_2| \gg |\rho_3| = |\rho_4| \approx |\rho_1|$, and ρ_1 (in contrast to ρ_2 and ρ_4) should have a negative sign, one may deduce that the observed reduction in $|a_{H(2)}|$ relative to the expected value is primarily due to the A -term. For the same reasons, an analogous reduction in $|a_{H(3)}|$ would arise mainly from one of the B' -terms. The angles required to attain a satisfactory agreement with the predicted values are estimated as $\varphi = 70-80^\circ$ and $\theta_{\mu\nu}, \theta_{\mu\nu'} = 65-75^\circ$; the latter estimates are consistent with the deviation of the ten-membered perimeter from planarity, as indicated by molecular models and established by X -ray analysis of 1,6-methano[10]annulene-2-carboxylic acid [16].

The sign of $a_{H(2)}$ should be negative, since the large *McConnell* term (-4 to -6 gauss) certainly predominates in this case. On the other hand, either sign can be advanced for $a_{H(3)}$; the negative Q -term and the sum of the positive A - and B' -terms must be here of similar magnitude (1 to 2 gauss) and almost cancel out. Attempts to measure the sign of $a_{H(3)}$ by NMR. spectroscopy have failed, because the direction of the 'Knight shift' for the 3, 4, 8, 9-protons in mixtures of II and II $^\ominus$ (2, 5, 7, 10-tetradeuterio derivatives of I and I $^\ominus$) [7] [21] could not be unequivocally determined [22].

Temperature dependent changes in geometry. We suggest that the marked temperature dependence observed for the coupling constants of the α - and β -protons in I $^\ominus$ is in both cases due to slight changes in geometry. Whereas for the β -protons such a

suggestion is readily substantiated by experience, it is less obvious in the case of the α -protons and requires some further supporting arguments.

The \cos^2 -function changes very little for angles close to 90° , but it becomes more sensitive for angles significantly deviating from this value. Thus an increase of 1° alters the \cos^2 -function by 0.0003, 0.0062 and 0.0114, when the pertinent angle is 90° , 80° , and 70° , respectively. Assuming the general validity of eq. (3), one therefore predicts that slight changes in the geometric parameters φ , $\theta_{\mu\nu}$ and $\theta_{\mu\nu}'$ should affect the α -proton coupling constants for I^\ominus to a much larger extent than the corresponding values for a planar π -radical. This prediction also holds with regard to variations in temperature, provided that such variations produce similar changes in geometry of both radicals.

Again, it is instructive to consider the α -proton coupling constants for I^\ominus and V^\ominus in which the relevant X -ray temperature factors are likely to be comparable⁹⁾. Examination of eq. (3) for I^\ominus with $\varphi = 70$ – 80° and $\theta_{\mu\nu}$, $\theta_{\mu\nu}' = 65$ – 75° shows that changes of 2 – 3° in these angles for a range of 100°C would suffice to produce the observed temperature dependence of the values $|a_{H(2)}|$ and $|a_{H(3)}|$. On the other hand, analogous changes for V^\ominus , with φ , $\theta_{\mu\nu}$, $\theta_{\mu\nu}' \approx 90^\circ$, would lead to variations in α -proton coupling constants which are smaller by one to two orders of magnitude, as found experimentally.

Final remarks. We conclude that the deviation of the ten-membered perimeter from planarity is not only responsible for the abnormally small values $|a_{H(\mu)}|$ but also indirectly for their marked temperature dependence. Because of this deviation, the coupling constants $a_{H(\mu)}$ are very sensitive to small changes in geometry, produced by variations of temperature¹⁰⁾.

INDO calculations [13] which have been referred to in the present paper confirm the sensitivity of the proton coupling constants to the slightest changes in the geometry of I^\ominus . They yield negative signs for $a_{H(2)}$ and $a_{H(3)}^{\text{CH}_2}$, in accordance with the predictions of the respective eqs. (3) and (2), and favour a positive sign in the case of $a_{H(3)}$. However, a quantitative agreement between the calculated and experimental values has not been so far achieved. We are planning to perform further calculations, in which the numerous geometry parameters are systematically varied, and hope to be able to report the results in the near future.

Appendix. The ^{13}C coupling constants for I^\ominus quoted on p. 2740 have not been given previously [1] and are therefore briefly considered in the present paper. Figure 9 shows the satellites at the low-field end of the spectrum, the analysis of which yields two coupling constants

$$|a_{C(2)}| = 6.9 \pm 0.1 \quad \text{and} \quad |a_{C(1)}| = 6.4 \pm 0.2 \text{ gauss}$$

for ^{13}C nuclei in four (2, 5, 7, 10) and two (1, 6) equivalent carbon centers, respectively. These assignments are based on the intensities of the satellites relative to those of the corresponding main lines, and on calculations by means of current formulae [24]. The latter predict a positive sign for $a_{C(2)}$ and a negative one for $a_{C(1)}$. They also indicate that the absolute values of the non-identified ^{13}C coupling constants, $a_{C(3)}$ (centers 3, 4, 8, 9) and $a_{C(3)}^{\text{CH}_2}$ should be only about 1 gauss.

⁹⁾ The X -ray analysis of naphthalene (V) [23] and the 2-carboxylic acid of I [16] point to comparable temperature factors in the two molecules. We thank Dr. M. Dobler of the ETH Zürich for supplying us with the X -ray data in a form suitable for a meaningful comparison.

¹⁰⁾ The considerable increase in $|a_{H(2)}|$ upon association of I^\ominus with the counter-ion (see Figure 5) can be interpreted, too, by the sensitivity of $a_{H(2)}$ to slight changes in geometry.

Studies of temperature dependence for $a_{C(2)}$ and $a_{C(1)}$ have been carried out in the range -120° to -30° (DME/Na $^\oplus$ as solvent/counter-ion). The observed changes are of the same order of magnitude as the experimental error.

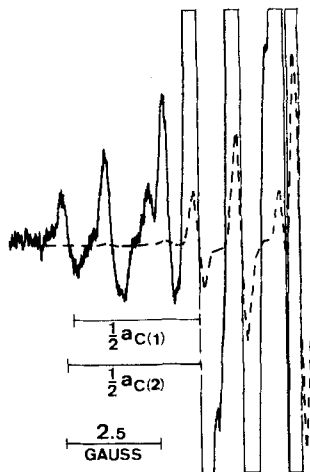


Fig. 9. The low-field end in the ESR. spectrum of I^\ominus

Solvent: DME; counter-ion: Na $^\oplus$; temp.: -90° ; low (---) and high (—) amplification of the signals

We thank Dr. J. Heinzer (now at Lab. für Organische Chemie der ETH Zürich) for taking some of the ESR. spectra reported in this paper. The work was supported by the Schweiz. Nationalfonds (Project No. SR 2.120.69).

BIBLIOGRAPHY

- [1] F. Gerson, E. Heilbronner, W. A. Böll & E. Vogel, *Helv.* **48**, 1494 (1965).
- [2] F. Gerson, "High Resolution ESR Spectroscopy", J. Wiley & Sons Ltd., New York, and Verlag Chemie, Weinheim, 1970.
- [3] F. Gerson & J. H. Hammons, "ESR Spectra of Radical Ions of Nonbenzenoid Aromatics" in Volume II of "Nonbenzenoid Aromatics" (J. P. Snyder ed.), Academic Press, New York, 1971, p. 81.
- [4] R. G. Lawler, J. R. Bolton, M. Karplus & G. K. Fraenkel, *J. chem. Physics* **47**, 2149 (1967).
- [5] F. Gerson, J. Heinzer & E. Vogel, *Helv.* **53**, 95 (1970).
- [6] T. R. Tuttle, Jr., *J. Amer. chem. Soc.* **84**, 1492, 2839 (1962); G. Vincow, M. L. Morrell, F. R. Hunter & H. J. Dauben, Jr., *J. chem. Physics* **48**, 2876 (1968).
- [7] E. de Boer & J. P. Colpa, *J. physic. Chemistry* **71**, 21 (1967).
- [8] H. M. McConnell, *J. chem. Physics* **24**, 632 (1956).
- [9] H.-R. Blattmann, W. A. Böll, E. Heilbronner, G. Hohlneicher, E. Vogel & J.-P. Weber, *Helv.* **49**, 2017 (1966).
- [10] A. D. McLachlan, *Molec. Physics* **3**, 233 (1970).
- [11] A. Carrington, *Quart. Reviews* **17**, 67 (1963); "Orbital Degeneracy and Spin Resonance in Free Radical Ions", Royal Institute of Chemistry, Lecture Series 1965; W. D. Hober, *J. chem. Physics* **43**, 2187 (1965); D. Purins & M. Karplus, *ibid.* **50**, 214 (1969).
- [12] L. Salem, "The Molecular Orbital Theory of Conjugated Systems", W. A. Benjamin Inc., New York-Amsterdam 1966.
- [13] J. A. Pople & D. L. Beveridge, "Approximate Molecular Orbital Theory", Mac Graw Hill Book Company, 1970.
- [14] F. Gerson, J. Heinzer & E. Vogel, *Helv.* **53**, 103 (1970).
- [15] J. R. Bolton in "Radical Ions", p. 9 (E. T. Kaiser & L. Kevan, eds.), Interscience Publishers, New York 1968.
- [16] M. Dobler & J. D. Dunitz, *Helv.* **48**, 1429 (1965).

- [17] C. Heller & H. M. McConnell, J. chem. Physics 32, 1535 (1960); A. Horsfield, J. R. Morton & D. H. Whiffen, Molec. Physics 4, 425 (1961).
 [18] F. Gerson, E. Heilbronner & B. Weidmann, Helv. 47, 1951 (1964); see also *op. cit.* [2], p. 107.
 [19] K. Markau & W. Maier, Z. Naturforsch. 16a, 636 (1961).
 [20] A. Berndt, Tetrahedron 25, 37 (1969); see also G. R. Luckhurst, Molec. Physics 11, 205 (1966).
 [21] E. de Boer & C. McLean, J. chem. Physics 44, 1334 (1966).
 [22] K. Müllen, Thesis, University of Basel, 1971.
 [23] D. W. J. Cruickshank, Acta cryst. 10, 504 (1957).
 [24] M. Karplus & G. K. Fraenkel, J. chem. Physics 35, 1312 (1961); M. T. Melchior, *ibid.* 50, 511 (1969).

290. Über den Verteilungssatz der Auxochrome bei Azokörpern IV. Azokörper mit zueinander *p*-ständigen Auxochromen

von K. Kokkinos und R. Wizinger

Institut für Farbenchemie der Universität Basel

(3. XI. 71)

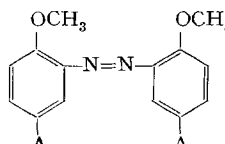
Summary. In azo compounds with CH₃O groups in *o*-position to the azo groups the introduction of the weak auxochromes CH₃- and CH₃O- into the *p*-position to the methoxy groups (*m*-position to the chromophor) causes relatively strong bathochromic effects, in conformity with the rule of repartition.

In unserer dritten Mitteilung [1] über den Verteilungssatz der Auxochrome bei Azokörpern wurde an einigen Derivaten des 2-Hydroxy-azobenzols und des 2-Hydroxy-4'-nitro-azobenzols gezeigt, dass – in Übereinstimmung mit dem Verteilungssatz – Auxochrome in *p*-Stellung zur Hydroxygruppe eine sehr beachtliche Farbvertiefung hervorrufen, trotzdem sie nicht in Konjugation mit dem Azochromophor stehen. Wir haben dieses Gebiet nun ein wenig weiter ausgebaut durch Einbeziehung von Azokörpern mit Methoxygruppen in 2-Stellung zur Azogruppe.

In der Reihe der symmetrischen 2,2'-Dimethoxy-azokörper standen uns zur Verfügung: 2,2-Dimethoxy-azobenzol (I), 2,2'-Dimethoxy-5,5'-dimethyl-azobenzol (II) und 2,2', 5,5'-Tetramethoxy-azobenzol (III).

Das 2,2'-Dimethoxy-azobenzol (I) stellten wir dar nach Starke [2] durch Reduktion von *o*-Nitro-anisol mit Zinkstaub in alkoholischer Natronlauge. Das 2,2'-Dimethoxy-5,5'-dimethyl-azobenzol (II) erhielten wir nach Brasch & Freyss [3] durch Kuppeln von diazotiertem 3-Amino-4-kresolmethyläther mit *p*-Kresol zu 2-Methoxy-2'-hydroxy-5,5'-dimethyl-azobenzol (IIa) und Methylierung des letzteren mit Methyljodid in alkalischer Kalilauge. Die Absorptionsspektren der drei Azokörper I, II und IIa waren noch nicht untersucht. Bezüglich des 2,2', 5,5'-Tetramethoxy-azobenzols (III) sei auf Mitteilung I [4] verwiesen.

Die Messungen in alkoholischen Lösungen ergaben für I, II und III:

	A	λ_{\max} in nm (log ϵ)
I	H-	312 (3,877), 368 (4,017)
II	CH ₃ -	314 (3,938), 381 (4,056)
III	CH ₃ O-	315 (3,809), 411 (3,890) ¹⁾

1) Bezüglich weiterer Details an den Absorptionsspektren s. Experimentelles.